



Cp*Ru⁺ complexes of benzylideneaniline and salicylideneaniline

Dale E. Wheeler^{a,*}, Nicholas W. Baetz^a, Grant N. Holder^a, Scott T. Hill^b,
Steven Milos^c, Kraig A. Luczak^d

^a *A.R. Smith Department of Chemistry, Appalachian State University, Boone, NC 28608, USA*

^b *Department of Chemistry, Alma College, Alma, MI 48802, USA*

^c *Northwestern Memorial Hospital, Chicago, IL 60611, USA*

^d *National Starch and Chemical Company, Bridgewater, NJ 08807, USA*

Received 13 June 2001; accepted 18 October 2001

Abstract

The reaction product of Cp*Ru(CH₃CN)₃⁺ OSO₂CF₃⁻ with salicylaldehyde yielded (**1**) which reacted with a series of aniline derivatives to produce air-stable solids. These products were characterized by ¹H and ¹³C NMR spectrometry and UV–Vis spectroscopy. Solvatochromism studies of these products revealed that the *p*-NH₂ and *p*-N(CH₃)₂ derivatives exhibit relatively large values of molecular hyperpolarizability and have the potential to exhibit nonlinear optical properties. These derivatives were further studied by electrochemical investigations. © 2002 Elsevier Science B.V. All rights reserved.

Keywords: Ruthenium; Benzylideneaniline; Salicylideneaniline; Nonlinear optical materials; Electrochemistry

1. Introduction

It is well established that aniline derivatives react with aromatic aldehydes to form imines [1], commonly called Schiff bases. Our previous studies [2] demonstrated facile reactivity of the formyl group in benzaldehyde upon coordination of the aromatic ring to a Cp*Ru⁺ moiety (Cp* = C₅Me₅). The enhanced electrophilic character of the formyl carbon is believed to be due to the electron withdrawing effect of the coordinated Ru(II).

Our interest in benzylideneaniline complexes having a single η⁶-coordinated Cp*Ru⁺ is their potential as nonlinear optical (NLO) materials. Basic features of NLO organometallic materials include the presence of a highly conjugated and polarizable π electron system and the occurrence of an intermolecular charge transfer band [3]. Extended donor/acceptor aromatic systems such as in benzylideneanilines [4] have demonstrated strong second harmonic generation characteristics shown to arise from the conjugated π electron system

bridging electron donor and acceptor groups. This article reports our efforts to increase the conjugation within these materials by reacting the salicylaldehyde complex Cp*Ru(η⁶-*o*-OH-C₆H₄CHO)⁺ OSO₂CF₃⁻ (**1**) with several aniline derivatives.

2. Experimental

All synthetic procedures were carried out under a dry nitrogen atmosphere with glassware fitted with Teflon solvent seal connections using standard Schlenk techniques. All solvents were freshly distilled prior to use. Methanol was dried over Mg/I₂, diethyl ether was dried over calcium hydride, methylene chloride was predried over P₂O₅, distilled, and dried over calcium hydride. 4-Hydroxyaniline, 4-chloroaniline, 1,4-phenylenediamine, and 4-methoxyaniline were purified by recrystallization prior to use. Salicylaldehyde, benzaldehyde, and aniline were distilled prior to use. 4-*N,N*-dimethylaminoaniline was purchased from Aldrich Chemical Co. and used without further purification.

Methylene chloride was used as the reaction solvent because of the solubility of the starting materials and products. Diethyl ether was used to precipitate the

* Corresponding author. Tel.: +1-828-262 6805; fax: +1-828-262 6558.

E-mail address: wheelerde@appstate.edu (D.E. Wheeler).

products from solution. Products were collected by filtration and dried under vacuum.

Synthetic procedures, ^1H and ^{13}C data for $\text{Cp}^*\text{Ru}(\eta^6\text{-C}_6\text{H}_5\text{CH}=\text{NC}_6\text{H}_4\text{OH-}p)^+ \text{OSO}_2\text{CF}_3^-$ (**13**), $\text{Cp}^*\text{Ru}(\eta^6\text{-C}_6\text{H}_5\text{CH}=\text{NC}_6\text{H}_4\text{Cl-}p)^+ \text{OSO}_2\text{CF}_3^-$ (**14**), and $\text{Cp}^*\text{Ru}(\eta^6\text{-C}_6\text{H}_5\text{CH}=\text{NC}_6\text{H}_4\text{NH}_2\text{-}p)^+ \text{OSO}_2\text{CF}_3^-$ (**15**) have been previously reported [2]. The procedure for the synthesis of $\text{Cp}^*\text{Ru}(\eta^6\text{-C}_6\text{H}_5\text{CHO})^+ \text{OSO}_2\text{CF}_3^-$ (**2**) was also previously reported [7].

The ^1H NMR spectra (Table 1) were measured at 300 MHz and ^{13}C NMR spectra (Table 2) at 75.5 MHz with a Bruker AC-F 300 FT NMR spectrometer at Appalachian State University. UV–Vis spectra (Table 3) were recorded on a Shimadzu Model UV 2401 Spectrophotometer at Appalachian State University.

Elemental analyses were performed by Galbraith Laboratories in Knoxville, TN.

2.1. $\text{Cp}^*\text{Ru}(\eta^6\text{-}o\text{-OHC}_6\text{H}_4\text{CHO})^+ \text{OSO}_2\text{CF}_3^-$ (**1**)

$\text{Cp}^*\text{Ru}(\text{NCCH}_3)_3^+ \text{OSO}_2\text{CF}_3^-$ (**1**) [7] (4.00 g, 7.87 mmol) was dissolved in 40 ml CH_2Cl_2 . Salicylaldehyde, $o\text{-OHC}_6\text{H}_4\text{CHO}$, (1.00 g, 8.19 mmol) was added to the solution and the mixture was stirred overnight resulting in a pale yellow solution. The solvent was removed under vacuum and 25 ml diethyl ether was added to the resulting solid. The mixture was stirred and then filtered and the cream colored powder was dried under vacuum. 3.53 g, 88% yield. *Anal.* Found: C, 42.12; H, 4.34. $\text{C}_{18}\text{H}_{21}\text{F}_3\text{O}_5\text{RuS}$. Calc.: C, 42.60; H, 4.17%.

Table 1
 ^1H NMR data

	Imine proton (1H, s)	Non-coordinated aromatic ring protons	Coordinated aromatic ring protons	Other protons		Cp* methyl protons (15H, s)
1			6.36 (1H, d, $^3J_{\text{HH}} = 6.3$ Hz) 6.02 (1H, d, $^3J_{\text{HH}} = 5.7$ Hz) 5.83 (1H, t, $^3J_{\text{HH}} = 5.8$ Hz) 5.63 (1H, t, $^3J_{\text{HH}} = 5.7$ Hz)	CHO	10.33	(1H, s) 1.89
3	8.33	7.34–7.36 (2H, m) 7.20–7.24 (3H, m)	6.42 (2H, d, $^3J_{\text{HH}} = 5.7$ Hz) 5.96–6.00 (3H, m)			1.87
4	8.42	7.32 (2H, d, $^3J_{\text{HH}} = 9.0$ Hz)	6.51 (2H, d, $^3J_{\text{HH}} = 6.3$ Hz)	OCH ₃	3.81	(3H, s) 1.91
5	8.36	6.92 (2H, d, $^3J_{\text{HH}} = 9.0$ Hz) 7.24 (2H, d, $^3J_{\text{HH}} = 9.0$ Hz)	5.96–6.06 (3H, m) 6.45 (2H, d, $^3J_{\text{HH}} = 5.7$ Hz)	N(CH ₃) ₂	2.99	(6H, s) 1.89
6	8.98	6.69 (2H, d, $^3J_{\text{HH}} = 8.1$ Hz) 7.35–7.45 (5H, m)	5.92–6.01 (3H, m) 6.64 (1H, d, $^3J_{\text{HH}} = 4.8$ Hz) 5.83 (1H, d, $^3J_{\text{HH}} = 5.1$ Hz) 5.77–5.72 (2H, m)			1.87
7	9.03	7.40 (5H, s)	6.64 (1H, d, $^3J_{\text{HH}} = 4.5$ Hz) 5.82 (1H, d, $^3J_{\text{HH}} = 5.1$ Hz) 5.77–5.72 (2H, m)			1.86
8	8.58	7.22 (2H, d, $^3J_{\text{HH}} = 8.7$ Hz)	6.16 (1H, d, $^3J_{\text{HH}} = 5.0$ Hz) 5.57–5.65 (3H, m)	OH	3.81	(1H, broad) 1.73
9	8.96	6.77 (2H, d, $^3J_{\text{HH}} = 9.0$ Hz) 7.47 (2H, d, $^3J_{\text{HH}} = 7.2$ Hz)	6.64 (1H, d, $^3J_{\text{HH}} = 5.0$ Hz) 5.68–5.77 (3H, m)	OCH ₃	3.83	(3H, s) 1.86
10	8.58	6.94 (2H, d, $^3J_{\text{HH}} = 7.2$ Hz) 7.21 (2H, d, $^3J_{\text{HH}} = 8.7$ Hz) 6.63 (2H, d, $^3J_{\text{HH}} = 8.4$ Hz)	6.18 (1H, m) 5.62–5.57 (3H, m)	NH ₂	3.61	(2H, broad) 1.76
11	8.86	7.44 (2H, d, $^3J_{\text{HH}} = 9.3$ Hz) 6.69 (2H, d, $^3J_{\text{HH}} = 8.7$ Hz)	6.56 (1H, d, $^3J_{\text{HH}} = 5.3$ Hz) 5.71–5.69 (2H, m) 5.61 (1H, m)	N(CH ₃) ₂	3.01	(6H, s) 1.84
12						
13	8.92	Pyrene (9H) 8.28, 8.25, 8.14–8.07 (m) 8.02–7.91(m)	6.35 (1H, d, $^3J_{\text{HH}} = 5.7$ Hz) 5.67–5.56 (3H, m)			1.76

All spectra were taken in 9:1 $\text{CDCl}_3\text{:CD}_3\text{OD}$. The internal reference of residual CHCl_3 was set equal to 7.24 ppm.

Table 2
¹³C NMR data

	Imine carbon	Non-coordinated aromatic ring carbons					Coordinated aromatic ring carbons (<i>i</i> -OH)					Cp* carbons	Other carbons
1						133.5	87.7	85.2	81.9	80.3	77.8	97.2, 10.3	CHO 190.5
3	155.5	149.0	129.3	127.6	120.8		93.5	88.0	87.6	86.2		97.5, 10.2	
4	152.1	159.8	142.0	123.1	114.8		94.5	88.0	87.8	86.2		97.5, 10.6	OCH ₃ 55.6
5	148.0	150.6	137.6	123.2	112.4		95.4	87.8	87.7	85.9		97.3, 10.7	N(CH ₃) ₂ 40.4
6	161.6	146.1	129.8	129.1	121.5	133.1	87.2	86.8	85.1	79.8	77.8	96.4, 10.2	
7	162.1	144.7	134.7	130.0	123.0	132.9	87.2	86.7	84.1	79.9	77.7	96.5, 10.2	
8	158.5	156.1	137.7	122.8	116.3	132.6	86.3	86.2	84.5	80.0	77.5	95.9, 10.1	
9	161.8	159.8	138.6	123.1	115.0	133.6	87.3	86.4	85.9	80.1	77.7	96.1, 10.1	OCH ₃ 55.6
10	154.0	148.1	136.0	122.9	115.3	133.2	86.3	86.0	84.5	80.4	77.4	96.0, 10.0	
11	154.0	151.0	134.0	123.3	112.6	133.6	87.0	86.0	84.5	80.6	77.7	95.8, 9.9	N(CH ₃) ₂ 40.6
12	159.2	139.7	131.5	131.2	130.7	132.1	86.4	85.9	84.8	80.7	77.3	96.2, 10.0	
		128.6	128.1	127.1	126.5								
		126.0	125.9	125.7	125.6								
		125.0	124.2	121.1	114.9								

Spectra for compounds **1**, **4**, **5**, **6**, **7**, and **11** were taken in CDCl₃ with the reference set to 77.00 ppm. Spectra for compounds **3**, **8**, **9**, and **10** were taken in 1:1 CDCl₃ and CD₃OD with the reference set to 77.00 ppm.

 Table 3
 UV–Vis spectral data

Compound	Solvent λ _{max}				Molar absorptivity constant (in CH ₃ OH)
	CH ₂ Cl ₂	C ₆ H ₅ Br	H ₂ O	CH ₃ OH	
3	329.7	330.3	*	324.5	3800
4	357.0	356.2	339.8	348.3	9700
5	429.6	422.4	382.6	411.3	19 000
6	328.5	328.8	*	319.9	8500
7	334.5	336.0	*	326.3	8900
8	357.2	354.8	*	345.5	11 300
9	360.3	360.2	*	341.5	10 800
10	396.0	391.1	*	367.4	9800
11	442.2	431.4	*	391.4	16 900
13	334.8	332.6	317.1	326.4	5700
14	354.1	352.8	340.9	353.1	10 400
15	387.6	386.7	362.5	387.1	15 400

*, λ_{max} was not observed in these solutions. Note: Absorbance values ranged from 0.5 to 1.0.

2.2. Cp*Ru(η⁶-C₆H₅CH=NC₆H₅)⁺ OSO₂CF₃⁻ (**3**)

Cp*Ru(η⁶-C₆H₅CHO)⁺ OSO₂CF₃⁻ (**2**) (0.172 g, 0.349 mmol) was dissolved in 20 ml of CH₂Cl₂. Freshly distilled aniline (20 drops, ca. 10 mmol) was added and the reaction was stirred for 4 h. Diethyl ether was added (ca. 15 ml) to the clear rose-colored solution until the precipitation of the product was complete. The white powdered solid was filtered and dried under vacuum, 0.14 g, 70% yield. *Anal.* Found: C, 50.43; H, 4.47. C₂₄H₂₆F₃N₃O₃RuS. Calc.: C, 50.88; H, 4.63%.

2.3. Cp*Ru(η⁶-C₆H₅CH=NC₆H₄OCH₃-*p*)⁺ OSO₂CF₃⁻ (**4**)

Cp*Ru(η⁶-C₆H₅CHO)⁺ OSO₂CF₃⁻ (**2**) (0.182 g, 0.369 mmol) was dissolved in 15 ml of CH₂Cl₂. *p*-

Methoxyaniline (0.0455 g, 0.369 mmol) was added and the reaction was stirred for 4 h. Diethyl ether was added (ca. 10 ml) to complete the precipitation of the product from the cloudy white solution. The resulting pale yellow powder was filtered and dried under vacuum, 0.17 g, 78% yield. *Anal.* Found: C, 49.84; H, 4.59. C₂₅H₂₈F₃N₃O₄RuS. Calc.: C, 50.33; H, 4.73%.

2.4. Cp*Ru(η⁶-C₆H₅CH=NC₆H₄N(CH₃)₂-*p*)⁺ OSO₂CF₃⁻ (**5**)

Cp*Ru(η⁶-C₆H₅CHO)⁺ OSO₂CF₃⁻ (**2**) (0.210 g, 0.427 mmol) was dissolved in 20 ml of CH₂Cl₂. *p*-*N,N*-dimethylaminoaniline (0.072 g, 0.53 mmol) was added and the reaction was stirred overnight. Diethyl ether was added (ca. 15 ml) to the dark green solution and a green solid precipitated from solution. The green pow-

der was filtered and dried under vacuum, 0.18 g, 70% yield. *Anal.* Found: C, 50.79; H, 5.01. $C_{26}H_{31}F_3N_2O_3RuS$. Calc.: C, 51.22; H, 5.13%.

2.5. $Cp^*Ru(\eta^6\text{-}o\text{-OHC}_6\text{H}_4\text{CH=NC}_6\text{H}_5)^+ OSO_2CF_3^-$ (**6**)

$Cp^*Ru(NCCH_3)_3^+ OSO_2CF_3^-$ (**1**) (0.203 g, 0.399 mmol) was dissolved in 20 ml of CH_2Cl_2 . Freshly distilled aniline (20 drops, ca. 10 mmol) was added and the reaction was allowed to stir overnight. The product was precipitated from the pale yellow solution by adding approximately 10 ml of diethyl ether. The white powdered solid was filtered and dried under vacuum, 0.18 g, 76% yield. *Anal.* Found: C, 49.06; H, 4.38. $C_{24}H_{26}F_3NO_4RuS$. Calc.: C, 49.48; H, 4.50%.

2.6. $Cp^*Ru(\eta^6\text{-}o\text{-OHC}_6\text{H}_4\text{CH=NC}_6\text{H}_4\text{Cl-}p)^+ OSO_2CF_3^-$ (**7**)

$Cp^*Ru(NCCH_3)_3^+ OSO_2CF_3^-$ (**1**) (0.198 g, 0.391 mmol) was dissolved in 20 ml of CH_2Cl_2 . *p*-Chloroaniline (0.0516 g, 0.405 mmol) was added to the solution of **1** and the reaction mixture was stirred for 4 h. Precipitation of the product from the pale yellow solution occurred as approximately 10 ml of diethyl ether was added to the reaction solution. The white powdered solid was filtered and dried overnight under vacuum, 0.20 g, 83% yield. *Anal.* Found: C, 46.33; H, 3.84. $C_{24}H_{25}ClF_3NO_4RuS$. Calc.: C, 46.72; H, 4.08%.

2.7. $Cp^*Ru(\eta^6\text{-}o\text{-OHC}_6\text{H}_4\text{CH=NC}_6\text{H}_4\text{OH-}p)^+ OSO_2CF_3^-$ (**8**)

$Cp^*Ru(NCCH_3)_3^+ OSO_2CF_3^-$ (**1**) (0.202 g, 0.398 mmol) was dissolved in 20 ml of CH_2Cl_2 . *p*-Hydroxyaniline (0.0460 g, 0.425 mmol) was added to the solution of **1** and the reaction mixture was stirred overnight. About 10 ml of diethyl ether was added to the golden colored reaction solution inducing the precipitation of a pale yellow powder. The product was filtered and dried under vacuum, 0.17 g, 72% yield. *Anal.* Found: C, 47.81; H, 4.26. $C_{24}H_{26}F_3NO_5RuS$. Calc.: C, 48.16; H, 4.38%.

2.8. $Cp^*Ru(\eta^6\text{-}o\text{-OHC}_6\text{H}_4\text{CH=NC}_6\text{H}_4\text{OCH}_3\text{-}p)^+ OSO_2CF_3^-$ (**9**)

$Cp^*Ru(NCCH_3)_3^+ OSO_2CF_3^-$ (**1**) (0.133 g, 0.263 mmol) was dissolved in 15 ml of CH_2Cl_2 . *p*-Methoxyaniline (0.0324 g, 0.263 mmol) was added to the solution of **1** and the reaction mixture was stirred overnight. Precipitation of the yellow product occurred as approximately 10 ml of diethyl ether was added to the golden brown solution. The bright yellow powder was filtered and dried under vacuum overnight, 0.13 g,

82% yield. *Anal.* Found: C, 48.70; H, 4.39. $C_{25}H_{28}F_3NO_5RuS$. Calc.: C, 49.01; H, 4.61%.

2.9. $Cp^*Ru(\eta^6\text{-}o\text{-OHC}_6\text{H}_4\text{CH=NC}_6\text{H}_4\text{NH}_2\text{-}p)^+ OSO_2CF_3^-$ (**10**)

$Cp^*Ru(NCCH_3)_3^+ OSO_2CF_3^-$ (**1**) (0.203 g, 0.401 mmol) was dissolved in 20 ml of CH_2Cl_2 . 1,4-Phenylenediamine (0.0437 g, 0.404 mmol) was added to the solution of **1** and the reaction mixture was stirred for about 4 h. The addition of about 10 ml of diethyl ether induced a green precipitate to form from the pale green solution. The yellow green powdered product was filtered and dried under vacuum, 0.18 g, 72% yield. *Anal.* Found: C, 47.92; H, 4.33. $C_{24}H_{27}F_3N_2O_4RuS$. Calc.: C, 48.24; H, 4.55%.

2.10. $Cp^*Ru(\eta^6\text{-}o\text{-OHC}_6\text{H}_4\text{CH=NC}_6\text{H}_4\text{N(CH}_3)_2\text{-}p)^+ OSO_2CF_3^-$ (**11**)

$Cp^*Ru(NCCH_3)_3^+ OSO_2CF_3^-$ (**1**) (0.204 g, 0.402 mmol) was dissolved in 20 ml of CH_2Cl_2 . *p*-*N,N*-dimethylaniline (0.074 g, 0.543 mmol) was added to the solution of **1** and the reaction mixture was stirred overnight. A green solid precipitated from solution as approximately 10 ml of diethyl ether was added to the dark green solution. The green powdered product was filtered and dried under vacuum for several hours, 0.18 g, 74% yield. *Anal.* Found: C, 49.55; H, 4.75. $C_{26}H_{31}F_3N_2O_4RuS$. Calc.: C, 49.91; H, 4.99%.

2.11. $Cp^*Ru(\eta^6\text{-}o\text{-OHC}_6\text{H}_4\text{CH=NC}_{16}\text{H}_9)^+ OSO_2CF_3^-$ (**12**)

$Cp^*Ru(NCCH_3)_3^+ OSO_2CF_3^-$ (**1**) (0.158 g, 0.310 mmol) was dissolved in 15 ml of CH_2Cl_2 . 1-Aminopyrene (0.069 g, 0.32 mmol) was added to the solution of **1** and the reaction mixture was stirred overnight. Precipitation of the product occurred as approximately 10 ml of diethyl ether was added to the reaction solution. The orange powdered product was filtered and dried under vacuum, 0.16 g, 73% yield. *Anal.* Found: C, 57.42; H, 4.11. $C_{34}H_{30}F_3NO_4RuS$. Calc.: C, 57.78; H, 4.28%.

3. Results and discussion

The first reported derivative exhibiting NLO properties was 4-nitro-4'-methylbenzylideneaniline [5]. The crystal structure of this compound revealed the molecule to be nearly planar [5] and had a SHG efficiency 100 times urea. 4-Dimethylamino-4'-nitrobenzylideneaniline and 4-nitro-4'-dimethylaminobenzylideneaniline also have near planar structures [6], which promote the maximum conjugation of the strong elec-

tron donating and accepting groups. This paper reports the synthesis of several air-stable benzylideneanilines of the general formula $\text{Cp}^*\text{Ru}(\eta^6\text{-C}_6\text{H}_5\text{CH=NC}_6\text{H}_4\text{X-}p)^+$ from the reaction of $\text{Cp}^*\text{Ru}(\eta^6\text{-C}_6\text{H}_5\text{CHO})^+$ (**2**) with various *p*-substituted anilines. These products would possess a polar extended conjugated π system if the η^6 -benzylideneaniline part of the complex was planar.

The results of solvatochromism studies of these complexes (see Table 3) are an indication of the molecular hyperpolarizability (β). Large values of β are associated with chromophores comprised of electron donors and acceptors linked by a conjugated π system. Our studies revealed that the benzylideneaniline complexes with the strongest electron donating groups ($\text{X} = \text{NH}_2$ (**15**) and $\text{N}(\text{CH}_3)_2$ (**5**)) are green and that (**15**) exhibited the greatest solvatochromism. The complexes where $\text{X} = \text{Cl}$ (**14**), or H (**3**), were white powders and exhibited little solvatochromism, indicating that the benzylidene ligand may not be planar.

To increase the probability of a planar ligand, an *o*-OH group was added to the aromatic aldehyde, which would allow the possibility of hydrogen bonding with nitrogen. This would fix the ligand into a planar configuration and promote greater delocalization of π electrons. These complexes would exhibit greater solvatochromism indicating a potentially greater SHG efficiency.

The salicylaldehyde complex $\text{Cp}^*\text{Ru}(\eta^6\text{-}o\text{-OH-C}_6\text{H}_4\text{CHO})^+ \text{OSO}_2\text{CF}_3^-$ (**1**) was synthesized using the published procedure of Fagen, et al. [7]. Reactions of (**1**) with a variety of aniline derivatives produced a series of products with the general formula $\text{Cp}^*\text{Ru}(\eta^6\text{-}o\text{-OH-C}_6\text{H}_4\text{CH=NC}_6\text{H}_4\text{X-}p)^+ \text{OSO}_2\text{CF}_3^-$. See Scheme 1.

Curiously, only one of the $-\text{NH}_2$ groups in 1,4-phenylenediamine reacted with (**1**), even when a 2:1 ratio of amine:aldehyde was used. It is believed that the second *p*-amino group is unreactive toward (**1**) due to a decrease in the nucleophilic character of the nitrogen lone pair electrons. The decrease in the electron density of the uncoordinated ring may be due to the loss of the available nitrogen lone pair upon reaction forming the

imine bond. Electron density in the uncoordinated ring may also decrease if the salicylideneaniline ligand is planar and the electron withdrawing effects of the ruthenium is felt throughout the entire delocalized π system. The solvatochromism properties of these complexes were determined (see Table 3).

3.1. Electrochemical studies

3.1.1. Voltammetric behavior

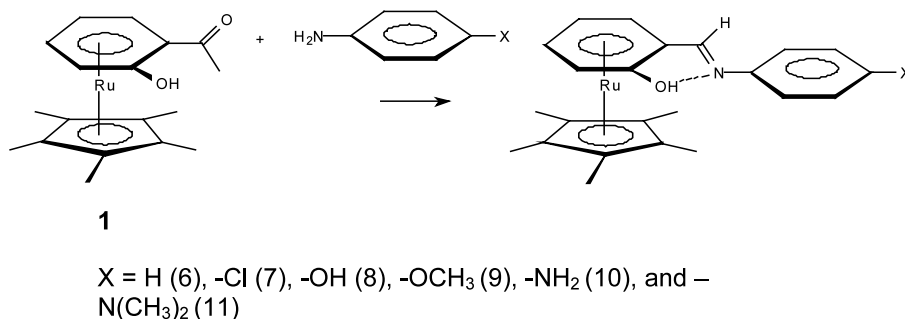
All compounds were examined on a BioAnalytical Systems, Inc. 100 B/W electrochemical workstation utilizing glassy carbon and platinum disk electrodes in acetonitrile (dried over CaH_2) and 0.1 M tetra-*N*-butylammonium hexafluorophosphate (TBAH) supporting electrolyte. All potentials are referenced to the Ag/Ag^+ couple and are uncorrected for liquid junction.

3.2. $\text{Cp}^*\text{Ru}(\eta^6\text{-}o\text{-OHC}_6\text{H}_4\text{CHO})^+ \text{OSO}_2\text{CF}_3^-$ (**1**)

Observed voltammetric processes consisted of two reductions at $E_{p,1} = -1.060$ V and $E_{p,2} = -1.920$ V. These potentials shifted cathodically with increasing scan rate and did not exhibit behavior characteristic of reversibility (anodic/cathodic current ratio < 1) at any scan rate up to 3 V s^{-1} . A wave at $E_{p,ox} = +1.080$ V, present only after scanning past $E_{p,2}$, represents the decomposition product of a chemical reaction following the second reduction and is also not reversible. This electroactive decay product decomposes slowly, as evidenced by the rapid diminution of $i_{ox}/i_{p,2}$ at scan rates $< 0.300 \text{ V s}^{-1}$. At scan rates $> 0.300 \text{ V s}^{-1}$, this ratio became constant within experimental error. Significant adsorption of the electroactive product formed from the reaction following E1 was observed.

3.3. $\text{Cp}^*\text{Ru}(\eta^6\text{-}o\text{-OHC}_6\text{H}_4\text{CH=NC}_6\text{H}_4\text{N}(\text{CH}_3)_2\text{-}p)^+ \text{OSO}_2\text{CF}_3^-$ (**11**)

The cyclic voltammogram for this compound is shown in Fig. 1a. Initial anodic scan exhibited a one-electron transfer at a half-wave potential $E_{ox,2} = 0.987$



Scheme 1. This scheme shows the general reaction of $\text{Cp}^*\text{Ru}(\eta^6\text{-}o\text{-OHC}_6\text{H}_4\text{CHO})^+ \text{OSO}_2\text{CF}_3^-$ (**1**) with various *p*-substituted anilines to give products **6–11**.

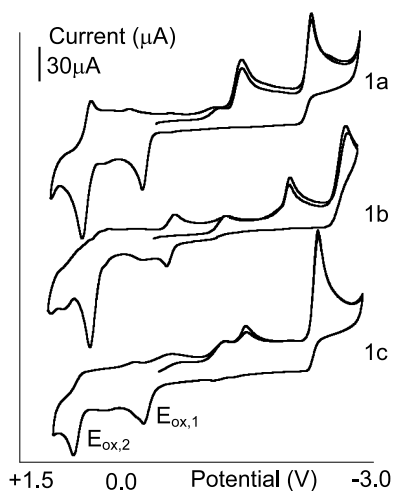


Fig. 1. Full cycle voltammetric scan (MeCN/0.1 M TBAH), glassy carbon electrode ($A = 0.109 \text{ cm}^2$) of: (a) **(11)**; (b) salicyl- N - C_6H_4 - N (Me)- p ; (c) **(10)**; Scan rates in all cases = 0.300 V s^{-1} .

V. The process is not fully reversible, though current ratios approached unity with increasing scan rates; separation between anodic and cathodic peak potentials (ΔE_p) was 0.130 V at 0.100 V s^{-1} and increases with scan rate. Initial cathodic scan reveals a non-reversible reduction at $E_{p,1} = -1.130 \text{ V}$, similar to that seen in **1**, as well as a reduction at $E_{p,2} = -2.050 \text{ V}$. A low-current reduction is observed at -0.845 V for all complexes. This amounts to a 'shoulder' on $E_{p,1}$ and may be a prepeak resulting from adsorption of the product of the chemical reaction following the -1.130 V reduction. Current magnitude for the first and second reductions do not show an equivalence, with $i_{p,1}$ between 0.55 and 0.65 of $i_{p,2}$. This is insufficient to justify the second reduction as a two-electron process. However, close examination of the second reduction shows a significantly different wavelshape than that displayed by the first reduction and characteristic of surface adsorption, which amply justifies the current inequities between the two processes. An oxidation, not observed on initial anodic scan, appeared at 0.190 V only after scanning through $E_{p,2}$. This is identical behavior to **1**, though the potential for the coupled peak ($E_{ox,1}$) is shifted cathodically by 0.900 V . This is the oxidation of a product of a rather slow chemical reaction following $E_{p,2}$. Current magnitude of $i_{ox,1}$ varies from 0.19 of $i_{p,2}$ (0.050 V s^{-1}) to equivalence at 2 V s^{-1} .

Comparison of the cyclic voltammetry of **(11)** with uncomplexed ligand salicyl= N - C_6H_4 - N (Me) $_2$ (Fig. 1b) indicates all electron-transfers are ligand based. The process $E_{ox,2}$ corresponds to electrochemical oxidation of the amino group on the uncoordinated ring. This oxidation approaches reversibility as scan rates increase, though ΔE_p approaches 0.250 V at 3 V s^{-1} . Current magnitude exhibited by the initial reduction is 0.46 – 0.6 that of the second reduction, though the sec-

ond reduction does not exhibit surface enhancement. However, the increase in current magnitude does not justify an assignment of two-electron stoichiometry, as current magnitude in that case must be 2.83 times higher than $i_{p,1}$. As for **(11)**, an oxidation coupled to $E_{p,2}$ appears, though shifted to -0.132 V , a cathodic shift of 0.320 V . Comparison of $i_{p,2}$ to the current of this coupled wave displays variation from 0.042 (0.100 V s^{-1}) to 0.5 (1 V s^{-1}). This indicates the chemical reaction following $E_{p,2}$ is much faster in the absence of RuCp*. Though the RuCp* moiety does not appear to be electroactive within our potential window, it does have an effect on the energy of the electron-transfer process. Compared with uncomplexed salicyl= N - C_6H_4 - N (Me) $_2$, there are anodic shifts between 0.500 and 0.700 V for both reductions, corresponding to a stabilization of the ligand LUMO following complexation of the RuCp* moiety. Potential differences between $E_{p,1}$ and $E_{p,2}$ for **(11)** and salicyl= N - C_6H_4 - N (Me) $_2$ are 0.920 V (complex) versus 0.750 V (salicyl= N - C_6H_4 - N (Me) $_2$), indicating the effect of RuCp* to be greater on $E_{p,1}$. This might indicate the first reduction corresponds to the ring/double bond system bound directly to the RuCp* while the latter is a ring-centered reduction of the uncoordinated ring. Interestingly, current ratios rise for the oxidation $E_{ox,2}$ following addition of RuCp*, indicating that the rate constant of the decomposition reaction following the oxidation of the dimethylamino nitrogen is lowered by the presence of RuCp*. An anodic shift of 0.120 V is observed for $E_{ox,2}$ following complexation. Kinetics of the chemical reactions following electron-transfer appear faster on Pt than glassy carbon as indicated by differences in the rate of change of current ratio with scan rate.

3.4. Cp*Ru(η^6 - o -OHC $_6$ H $_4$ CH= N C $_6$ H $_4$ NH $_2$ - p) $^+$ OSO $_2$ CF $_3^-$ (**10**)

The substitution of amino—for dimethylamino—results in a marked increase in the rate of decomposition following oxidation of amino moiety, as $E_{ox,2}$ exhibits much lower current ratios at any scan rate. (Fig. 1c). Other electron-transfer processes seemed unaffected save for a shift of about 0.050 – 0.100 V relative to the dimethylamino derivative; $E_{ox,2} = 1.085 \text{ V}$, $E_{p,1} = -1.150 \text{ V}$, $E_{p,2} = -2.100 \text{ V}$. One would expect peak shifts on the basis of inductive effect to be in an anodic direction for **11** relative to **10**. Cathodic and anodic peak potentials shift in opposing directions, with all electron-transfers shifting to more extreme values; this indicates a difference in electron-transfer mechanism related to the active hydrogens of the amine group. The $-NH_2$ functionality can give rise to proton transfers not possible for the $-N$ (Me) $_2$ group.

3.5. $Cp^*Ru(\eta^6-C_6H_5CH=NC_6H_4N(CH_3)_2-p)^+ OSO_2CF_3^-$ (**5**)

The effect of the highly active –OH group was examined by comparing the voltammetry of **11** and **5**, two compounds which differ only by the presence or absence of the hydroxyl group attached to the metalated ring. The reductive mechanism (Fig. 2a) is far more complex than **11**, probably due to the loss of stabilization provided by H-bonding between the imine nitrogen and the hydroxyl group. Removal of –OH results in a disproportionately large-magnitude reduction at $E_{p,3} = -1.570$ V followed by fast decomposition to multiple electroactive products. Processes $E_{p,1}$ and $E_{p,2}$ show similar peak potentials to **11**. Two additional processes are observed ($E_{p,4} = -2.092$ and $E_{p,5} = -2.188$ V),

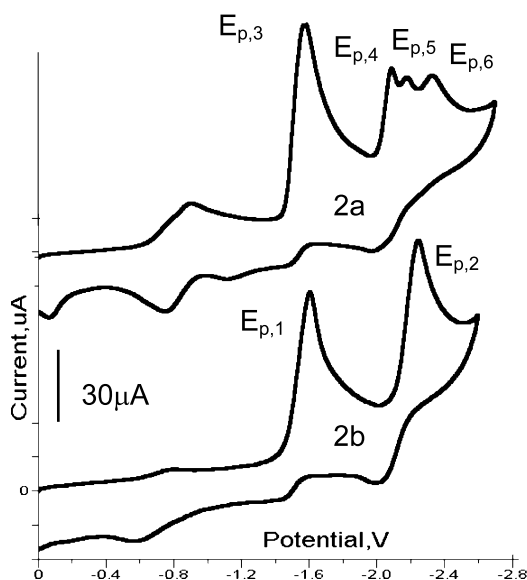


Fig. 2. Reductive voltammetry (MeCN/0.1 M TBAH) of: (a) **5**; and (b) **15**. Scan rate = 0.300 V s^{-1} .

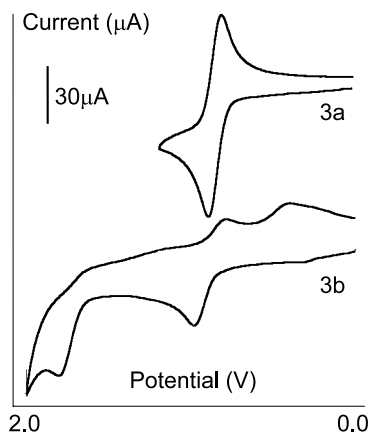


Fig. 3. Oxidative voltammetry (MeCN/0.1 M TBAH) of: (a) **5**; and (b) **15**. Scan rates in all cases = 0.300 V s^{-1} .

corresponding to the reduction of products formed following decomposition of the anion $E_{p,3}$. The current magnitudes of $E_{p,4}$ and $E_{p,5}$ decrease with increasing scan rate, indicating the scan is outrunning the reaction in which these products are formed and, therefore, that the rate constant for the formation of these processes is relatively slow on the voltammetric time scale. The first reduction appears more reversible than the corresponding process in **11**. The narrow shape of the forward wave of $E_{p,3}$ and its large magnitude ($i \propto v$) are indicative of moderate adsorption on the electrode surface. This is observed only on glassy carbon; the voltammetric curve has the characteristic diffusion-controlled shape on platinum as well as a magnitude similar to the other electron-transfer processes ($i \propto v^{1/2}$) [8]. On platinum, two non-reversible reductions were observed at $E_{p,4} = -1.560$ and $E_{p,5} = -2.246$ V. That these processes are observed only on glassy carbon implies their formation depends on some surface chemical process or these are strongly adsorbed products of a reaction following E_3 . Anodically, (Fig. 3a) the first oxidation shows excellent reversibility at all scan rates, intimating the significant function of –OH in the chemical decomposition following oxidation.

3.6. $Cp^*Ru(\eta^6-C_6H_5CH=NC_6H_4NH_2-p)^+ OSO_2CF_3^-$ (**15**)

The reduction of this compound (Fig. 2b) exhibits two waves of equal current magnitude at $E_{p,1} = -1.620$ and $E_{p,2} = -2.250$ V. The most extreme reduction shows some reversibility, unlike processes at similar potentials in **10** and **5**. $E_{p,1}$ and $E_{p,2}$ behavior is typical of the electrochemical ‘ECE’ mechanism. Ligand-based reduction (radical anion formation) is immediately followed by bond cleavage. The reversible reduction at -2.250 V is typical of a ring-based one-electron reduction [9]. Anodically (Fig. 3b), two oxidations of equal current magnitude are observed at $E_{ox,1} = 0.896$ and $E_{ox,2} = 1.805$ V. The first oxidation does not exhibit the same degree of reversibility as **5**; there is an obvious following chemical reaction to produce at least one electroactive product sufficiently long-lived to be reduced at 0.413 V. Diagnostic criteria for the first oxidation are essentially the same as **10**, emphasizing the reactivity of the oxidized—amino moiety compared with the—dimethylamino derivative. Reduction of **15** parallels **5** in the appearance of a reduction of $E_{p,3} = -1.620$ V which is absent in the salicyl derivative. As this potential is shifted cathodically by 0.040 V relative to **5**, a direction in opposition to expectations, one must suspect surface or intermolecular effects. Current magnitude for this reduction is much reduced on glassy carbon compared with corresponding process in **5**, leading one to the conclusion that the potential of the dimethylamino—derivative is

being lowered by substantial adsorption onto the electrode surface.

4. Summary of electrochemical results

One can deduce from the observations that:

- (a) The compounds exhibit ligand-based electron-transfers only.
- (b) Initial reductions are followed by chemical reactions, with some of the reactive fragments generated by bond cleavage from formed radical anions sufficiently long lived to be oxidized at scan rates $> 0.300 \text{ V s}^{-1}$; the hydroxyl moiety appears to prevent electrochemical reduction of the double bond possibly through H-bonding with the imine nitrogen.
- (c) The oxidation at approximately 900–1000 mV is due to the amine on the uncoordinated ring. Once oxidized, **10** decomposes much more quickly than **5** due to the ease with which H^+ is lost from the $-\text{NH}_2$ group.
- (d) Pronounced adsorption occurs in the absence of the hydroxyl group. Voltammetric behavior is more complex on glassy carbon electrode than platinum.

The complete electron-transfer mechanisms for these compounds will be presented in full in a future publication.

5. Conclusions

The facile reaction of $\text{Cp}^*\text{Ru}(\eta^6\text{-}p\text{-OHC}_6\text{H}_4\text{CHO})^+\text{OSO}_2\text{CF}_3^-$ (**1**) with a variety of aniline derivatives and primary amines yields air-stable solids. Solvatochromism studies of these products revealed that the $-\text{NH}_2$ and $-\text{N}(\text{CH}_3)_2$ derivatives, (**10**, **11**) exhibit the greatest change in λ_{max} between solvents. Large values of $\Delta\lambda_{\text{max}}$ indicate potential molecular hyperpolarizability within the compounds. Therefore, products (**10**, **11**) are the most likely in this series of complexes to exhibit nonlinear optical properties. Further studies of these complexes are ongoing.

Acknowledgements

We thank Johnson–Matthey for their generous loan of $\text{RuCl}_3 \cdot x \text{H}_2\text{O}$ through participation in their Metal Loan program. We also thank Appalachian State University for their monetary support of this project.

References

- [1] S. Patai, *The Chemistry of the Carbon–Nitrogen Double Bond*, Wiley, New York, 1970, pp. 64–83.
- [2] D.E. Wheeler, S.T. Hill, S. Milos, J.D. Williams, J.D. Johnson, *J. Organometallic Chem.* 530 (1997) 83.
- [3] (a) J.W. Perry, in: S.R. Marder, J.E. Sohn, G.D. Stucky, (Ed.), *Materials for Nonlinear Optics—Chemical Perspectives*, ACS Symposium Series 455, American Chemical Society, Washington, DC, 1991, pp. 67–88;
(b) D.F. Eaton, in: S.R. Marder, J.E. Sohn, G.D. Stucky, (Ed.), *Materials for Nonlinear Optics—Chemical Perspectives*, ACS Symposium Series 455, American Chemical Society, Washington, DC, 1991, pp. 128–156;
(c) J.-M. Lehn, in: S.R. Marder, J.E. Sohn, G.D. Stucky, (Ed.), *Materials for Nonlinear Optics—Chemical Perspectives*, ACS Symposium Series 455, American Chemical Society, Washington, DC, 1991, pp. 436–445.
- [4] (a) S.A. Jenekhe, C.-J. Yang, H. Vanherzele, J.S. Meth, *Chem. Mater.* 3 (1991) 985;
(b) J. Zyss, in: J.L. Bredas, R.R. Chance (Eds.), *Journal of Conjugated Polymeric Materials: Opportunities in Electronics, Optoelectronics, and Molecular Electronics*, Kluwer Academic Publishers, The Netherlands, 1990, p. 545;
(c) J.C. Dubois, in: J.L. Bredas, R.R. Chance (Eds.), *Journal of Conjugated Polymeric Materials: Opportunities in Electronics, Optoelectronics, and Molecular Electronics*, Kluwer Academic Publishers, The Netherlands, 1990, p. 321;
(d) J.F. Wolfe, S.P. Ermer, S.M. Lovejoy, D.S. Leung, K.P. Aron, G.A. Hansen, S.P. Bitler, in: *Nonlinear Optical Properties of Polymers*, Materials Research Society Symposium Proceedings 173, Materials Research Society, Pittsburgh, 1990, 499.
- [5] O.S. Filipenko, V.D. Shigorin, V.I. Ponomarev, L.O. Atovmyan, Z.S. Safina, B.L. Tanopol'skii, *Sov. Phys. Crystallogr.* 22 (1977) 305.
- [6] F. Skrabal, J. Straiger, H. Zollinger, *Helv. Chim. Acta* 58 (1975) 800.
- [7] P.J. Fagen, M.D. Ward, J.C. Calabrese, *J. Am. Chem. Soc.* 111 (1989) 1698.
- [8] R.S. Nicholson, I. Shain, *Anal. Chem.* 36 (4) (1964) 706.
- [9] C.P. Andrieux, J.-M. Saveant, R.T. Tallec, C.J. Tardy, *Am. Chem. Soc.* 1997, 119, 2424; and many others.